

## Advanced acoustic signal analysis used for wheel-flat detection

Pawel Komorski<sup>a\*</sup> , Grzegorz M. Szymanski<sup>a</sup> , Tomasz Nowakowski<sup>a</sup> , Malgorzata Orczyk<sup>a</sup> 

<sup>a</sup>Poznan University of Technology, Division of Railway Transport, Piotrowo 3 Street, 61-138 Poznań, Poland. E-mail: pawel.komorski@put.poznan.pl, grzegorz.m.szymanski@put.poznan.pl, tomasz.nowakowski@put.poznan.pl, malgorzata.orczyk@put.poznan.pl

\*Corresponding author

<https://doi.org/10.1590/1679-78256086>

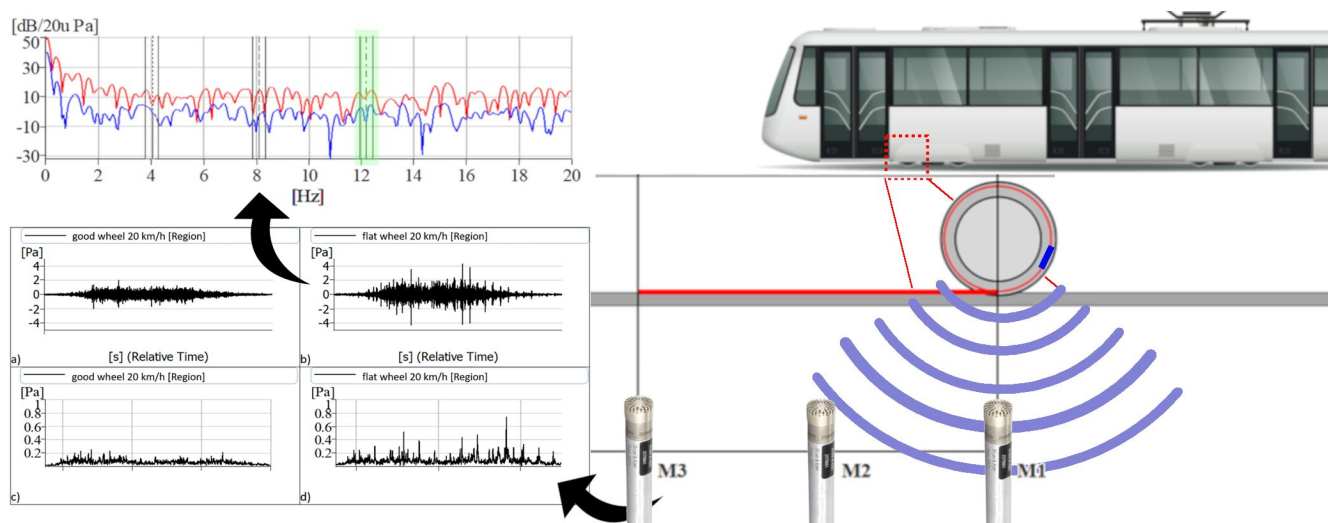
### Abstract

One of the most important aspects in the operation of rail vehicles is the implementation of transport while ensuring safety and comfort of passengers. Technical condition of the wheel rolling surfaces has a direct impact on these factors. These elements are subject to wear and tear in a continuous and discrete form. One of the discrete wear forms is the wheel-flat on wheel rolling surfaces that generate impulse noise. This translates into a significant deterioration of vibroacoustic comfort, and in extreme cases also to a greater risk associated with e.g. derailment of the vehicle. Therefore, it is desirable in particular by the rolling stock operator to carry out cyclic diagnostics and monitoring of the condition of wheel rolling surfaces. This paper is a continuation in a series of research articles carried out by the authors related to vibroacoustic diagnostics of wheel rolling surfaces in light rail vehicles. As part of this article, acoustic measurements were carried out at a dedicated track-side system during so-called pass-by tests. Acoustic signals were analyzed in accordance with the Fourier and Hilbert transforms. Additionally, the main assumptions of vibroacoustic diagnostics and analyses of point measures were used. This allowed for the development of yet another way of monitoring the occurrence of the problem of wheel flats in rail vehicles.

### Keywords

Tram rolling noise, wheel-flats, acoustic diagnostics, Hilbert transform

### Graphical Abstract



Received: April 24, 2020. In Revised Form: November 18, 2020. Accepted: November 19, 2020. Available online: January 08, 2021.

<https://doi.org/10.1590/1679-78256086>



Latin American Journal of Solids and Structures. ISSN 1679-7825. Copyright © 2021. This is an Open Access article distributed under the terms of the Creative Commons Attribution License, which permits unrestricted use, distribution, and reproduction in any medium, provided the original work is properly cited.

### 1 INTRODUCTION AND MAIN THEORETICAL ASPECTS

The good technical condition of the rolling wheel surface is one of the most important aspects of the rail running gear. Every rail vehicle in normal operating conditions has a standardized wheel rim profile. Therefore, all kinds of changes related to wear or damage of the wheel rolling surface have a negative impact on the vibroacoustic comfort and ride safety. Brief review of different wheel defects is presented in Figure 1. The flat wheel, which is included in the tread surface group defects, is one of the railway operational problems, where the local rolling surface geometry is changed significantly. Blocked wheel rotation is the main cause of this problem. It is caused by exceeding the adhesion forces of the wheel to the rail as a result of (in the most cases): rapid or emergency brake application, lack of brake release (especially in long freight trains) or presence of various undesirable materials (e.g. wet leaves) between wheel and rail contact point. At that moment the wheel surface temporarily slides over the rail which results an intensive abrasion of the rolling surface. As a consequence, the wheel profile is worn. Other wheel surface defects are the spalling effects. They are caused by peeling of the top wheel surface layer as a result of the material shifting from the flat wheel. The schematic of rolling surface damage is presented in Figure 2. Furthermore, the authors described the mathematical model of the flat wheel during rotation where the most important equation is as follows (Nowakowski et al., 2019):

$$m_z \cdot \left( l \left( \frac{\omega_0}{2} + \sqrt{\frac{g}{2R}} \right) \right) = \int_{t_0}^{t_0+\tau} F dt \tag{1}$$

It can be concluded that the value impulse force  $F$  during the dynamic wheel-rail interaction mostly depends on the reduced mass  $m_z$ , the wheel rotational speed  $\omega_0$ , the wheel diameter  $R$  and the wheel-flat length  $l$ . Moreover, dynamic track response is also dependent on the vehicle load and its suspension type, vertical and horizontal track stiffness, rail supporting system and also technical condition of the vehicle and track. Important information related to the dynamic response of the track to impulse phenomena from the rail vehicle is described in (Thompson, 2008). It presents the factors affecting the quality of the wheel-rail contact describing the influence of a wheel-flat on contact forces. The influence of the track construction on the vibrations damping in the track was indicated. The effect of wheel-flat on the level of vibrations generated by light rail vehicles has been presented in numerical study in (Alexandrou et al., 2016). It has been shown that damage longer than 3 cm significantly changes the quantitatively characterized vibrations during a tram ride. The paper (Jing, 2018) discusses the influence of train speed, length of a flat spot and axle load on the wheel-rail impact reactions. It has been shown that with an increase in the length of flat spot, the maximum impact force, the von Mises equivalent stresses and the XY shear stresses increase, and the maximum equivalent plastic strains decrease accordingly. The paper (Kouroussis et al., 2015) presents an analysis of the influence of the technical condition of the track and the vehicle on the generated vibrations. It was shown that the vibrations generated by the flat wheel may be several times smaller than those caused by local rail damage. It is therefore reasonable to observe the vibrations as close as possible to the wheel-rail contact. The work (Nowakowski et al., 2019) also presents the impact of wheel-flat on the generated rail vibrations. The results of cross-correlation of vibration signals from the rail indicate the validity of the location of the measurement points near the wheel-rail contact. In the (Stypuła, 2001), the impact of wheel-flat in metro on generated paraseismic vibrations was presented, considering the influence of track stiffness and vehicle load on the observed vibrations.

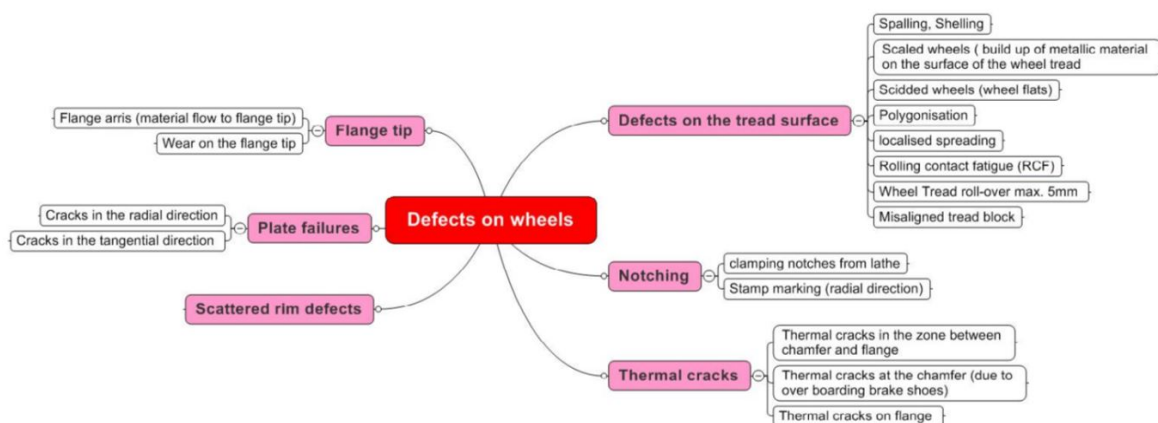
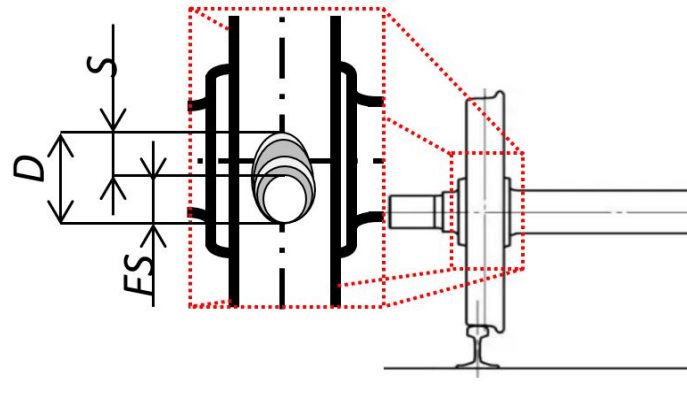


Figure 1 Wheel defects brief review (Behr, 2013)



**Figure 2** Wheel-flat example: D – wheel defect on wheel tread, FS – flat spot, S – spalling

The wheel-flat size can also be defined by the internal regulations of rail operators and owners. However, in tram vehicles management in Poland, there are no such rules and every urban operator has to deal with the problem on his own. On the other hand, there is one main European railway regulation which describes different kind of wheel defects, including the wheel-flats. The boundary lengths of the defects on the tread surface are presented in Table 1 (in accordance with EN 15313 standard). These maximum values are mainly related to train speed, axle load and wheel diameter conditions.

**Table 1** Boundary lengths of the defects on the tread (flats) (Behr, 2013; Standard, 2016)

M	M ≤ 18			18 < M ≤ 22,5				22,5 < M			
	V	V ≤ 160	160 < V ≤ 200	V < 200	V ≤ 120	120 < V ≤ 160	160 < V ≤ 200	200 < V	V ≤ 100	100 < V ≤ 120	120 < V
d	1000 < d	80	60	40	80	60	50	35	X	X	X
	840 < d ≤ 1000	60	50	30	60	50	35	25	60	50	30
	630 < d ≤ 840	40	30	25	40	30	25	20	40	X	X
	550 < d ≤ 630	35	25	X	X	X	X	X	X	X	X
	d < 550	30	X	X	X	X	X	X	X	X	X

M – axle load in tonnes (t); X – reserved (no known use); d – actual wheel diameter (mm); V – train speed (km/h)

The Polish State Railways and their internal standards are another good example where the wheel-flat is determined by the limit length values which cannot be exceeded (Polish National Railways Directorate, 2000). However, it is more simplified in comparison to EN 15313 standard:

- up to 60 mm for wheels with a diameter of 630 mm,
- up to 30 mm for wheels with diameter < 630 mm.

After exceeding the limit values, the wheels are sent for reprofiling. However, the wheel-flat searching process is the main problem (e.g. time consuming) and it is dependent on operator's experience.

Rolling surface defects lead to cyclical and sudden impacts during each wheel rotation on rail. Then the vibroacoustic comfort of the ride is significantly reduced and the impulse noise phenomenon occurs, which increases the overall rolling noise (Thompson, 1996 and 2008; Wu and Thompson, 2003). It is particularly burdensome in urban areas and cities. The wear of the rolling stock and infrastructure is another negative effect which is translated into increasing operational costs of servicing and using rail and tram network. A detailed description of the running surface wear curve (both wheel and rail) as an operating time function is provided in (Nowakowski et al., 2019). What is more important, this kind of defect increases the risk of rail vehicle derailment. Therefore, it is necessary to systematically monitor and diagnose the wheels technical condition. Given the impulse nature of the phenomenon, vibroacoustic signals seem to be a very good diagnostic parameter. Diagnostic and monitoring process (the system localization) can be carried out from the vehicle and also from the point of view of track. In both cases, an indispensable element is a mobile system for vibroacoustic measurements. Also, the diagnostician's experience in data analysis and selected research methods is crucial.

## 2 WHEEL-FLAT DETECTION METHODS, ALGORITHMS AND SYSTEMS

There are many different methods and systems for wheel-flat detection. However, most of them are prototypes based on some interesting ideas and analysis. Firstly, the monitoring methods can be divided into the stationary which means the measurement devices are located near the track. It is a very good idea for railway and tramway depots where only one diagnostic system is required and plenty different vehicles operate each day. The second monitoring method is the mobile one where the diagnostic system is installed on each vehicle (on-board systems). It is also a good idea; however, it could be more expensive for operator and depends on number of vehicles in the fleet.

For the purposes of this article mostly the stationary (wayside track) methods, algorithms and systems will be discussed. There are two commercial wheel-flat detection systems installed in several Polish cities. The WF system is located in the tram depot in Cracow (Madejski, 2006) and it is based on vibration signals measured by two transducers placed on the rail. It is a commercial system which is provided by GRAW Company (Germany). A simple detection method uses the impact vibration values which are higher when the flat wheel occurs. The second system called Revenga FWD (Flat Wheel Detector) is installed in the Poznan, Warsaw and Szczecin tram depots in Poland. The rail load (measured by several force sensors) is a main diagnostic parameter where limit values are monitored. A similar solution based on load measurement was used in the article (Meixedo et al., 2015). The Grupo Revenga from Spain is the system producer which is also a world's provider of different railway inspection systems.

Vibration track measurements is also used (Belotti et al., 2006; Krummenacher et al., 2017). The complex processing signal methods and algorithms are used in these two papers. The discrete wavelet transform and wavelet coefficient analysis in the first one are adapted, which makes it an effective method for rail wheel-flat detection in normal pass-by conditions. The second article presents another useful method where a machine learning analysis is implemented. Vibration complex methods are also popular in on-board systems where accelerometers are located on axle boxes or bearings, e.g. (Jia & Dhanasekar, 2007; Liang et al., 2013; Li et al., 2017). Unfortunately, many of them are only ideas and have not been used in real conditions.

Also very popular are other techniques like ultrasonic (Brizuela et al., 2011) and Doppler (Brizuela et al., 2010) methods. However the methods are characterized by some limitations (e.g. low train speed or some assessment errors). A new interesting method is proposed by (Roveri et al., 2015). They used the fibre Bragg grating sensors located along the track to monitor among others wheel wear. However it is only the experimental approach which still needs few improves. Other wheel-flat detection methods and systems are presented in (Alemi et al., 2016). The article is a literature review for different kinds of condition monitoring approaches in this topic.

In (Nowakowski et al., 2019) the wheel-flat detection algorithm is presented. The vibration signal and the Hilbert transform method were used for processing. The purpose was achieved with high effectiveness and it was shown that vibration signals combined with the envelope analysis is a well-founded solution. The Hilbert transform and other complex signal processing methods are also presented by (Bracciali et al., 1997; Zhang et al., 2018). In the second research case, authors have shown the fault detection from wayside acoustic signals emitted by train bearings. Furthermore, the authors (Komorski et al., 2018) elaborated the wheel-flat algorithm based on the JTFA (Joint Time-Frequency Analysis) method in acoustic signals processing. However in this case to achieve the goal, the tram passing speed should be more than 30 km/h which could be problematic (e.g. for some small depots). The last step of the general scientific investigation was to combine these two papers and create the novel wheel-flat detection algorithm using advanced acoustic signal analysis. The article is an extended version of the article presented at the international conference in 2019 called Dynamical Systems – Theory and Applications (Komorski et al., 2019) which consisted of acoustic measurements during trams pass-by tests (a few trams occurred with flat wheels) and experimental research using envelope analysis and Hilbert transform. The Hilbert transform usage has many advantages in processing different kinds of signals including acoustic signals analysis, especially in engineering applications (Luo et al., 2009). It allows to determine the real and imaginary parts of an analytic function (Feldman, 2011; García-Macías and Martínez-Castro, 2020; Luo et al., 2009; Skudrzyk, 1971). The analytic signal is created by implementing the Hilbert transform which enables to elaborate the instantaneous magnitude (so-called envelope) of the original time signal. Moreover, the frequency analysis can be done by finding out the instantaneous phase of the analytic signal. Therefore, the dynamic characteristics of a linear and non-linear system can be identified. The infinite Hilbert transform equation is described (Cempel, 1993; Feldman, 2011; Skudrzyk, 1971):

$$H[x(t)] = \tilde{x}(t) = \frac{1}{\pi} \int_{-\infty}^{\infty} \frac{x(\tau)}{t-\tau} d\tau \quad (2)$$

where the  $x(t)$  is a real measured acoustic signal in time domain,  $\tau$  is a time period before the transformation,  $t$  is a time period after the transformation and  $*$  denotes the Cauchy's principal value. As can be observed the Hilbert transform is not an integral between different domains, such as Fourier or Laplace, which can be another benefit in some research cases (Luo et al., 2009). In the (García-Macías and Martínez-Castro, 2020), authors have shown the example of the Hilbert transform and envelope usage in railway field. They proposed a model (based on Hilbert transform and semi-analytic method) for fast assessment of design envelopes of railway bridges. Main advantages of their solution for the moving-load induced-vibration problem of linear bridge structures are computational time reduction and high calculation accuracy. Another example is described in the (Kim et al., 2020) where authors have used the Hilbert transform and wavelet decomposition in railway wheel-flat defect prediction. However, in this case the vibration signals were measured on the vehicle axle box. So, it is a good example of the on-board diagnostic system in contrast to main aim of this research. The last but not least, in the (Tomlinson, 1987) author investigated the damage detection using the Hilbert transform in case of frequency response functions (FRF) analysis and their deviations. Considering these advantages, authors used the Hilbert (and also Fourier) transform to process the acoustic signals in case of novel wheel-flat detection algorithm.

### 3 EXPERIMENTAL RESEARCH METHODOLOGY

#### 3.1 Main Assumptions

The acoustic measurements during several pass-by tests on Franowo tram depot (Poznan, Poland) were the main part of the experimental research. The measurement equipment was located near one of the main tracks where all types of trams returning from service passed through. It is a good monitoring spot for track-side diagnostic system based on vibroacoustic signals. The tram speed was about 20-40 km/h. The main goal of the measurements was to develop a basis for the diagnostic method to identify wheel-flats using acoustic signals and advanced analysis techniques.

#### 3.2 Measurement points and research objects

From the recordings of signals from trams operated in the depot, trams with a wheel-flat were selected, which were the objects of research. The one where the wheel-flat occurred was Moderus Beta MF AC BD tram. Defect surface on the wheels treads was ellipse-shaped and was equal to 66 mm (length) and 32 mm (width). The reference signal representing wheels in good condition was recorded also during the passage of this type of tram. The main vehicle technical parameters are listed in Table 2. The track was ballasted and constructed from a 60R2 rail type placed on the Moll sleepers which is in accordance with EN 14811 regulation (Standard, 2019).

**Table 2** The main vehicle technical parameters as a research object

Technical parameters	Description
Manufacturer	Modertrans Poznan
Model	Moderus Beta MF AC BD
Length	28250 mm
Width	2350 mm
Tram segments number	3
Tram joints number	2
Motor bogies number	4
Trailer bogies number	0
Percentage of low floor	25%
Motor engine number	8 (41.5 KW each one)
Maximum speed	70 km/h
Min/Max wheel diameter	600/654 mm

The measurement position as a scheme is shown in Figure 3. Three microphones (M1-M3) were used, located at the distance of 2000 mm from the external rail.

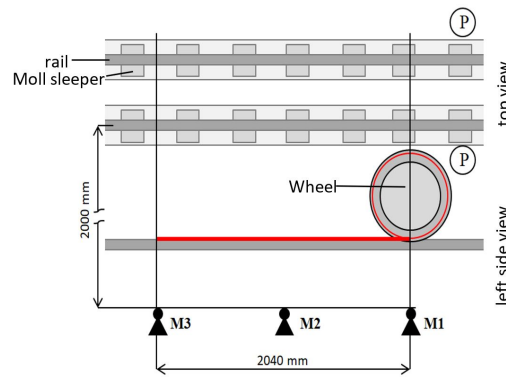


**Figure 3** The scheme of measuring position during acoustic pass-by tests; M1-M3 – Microphones, P – Photocells

The microphones were spread along the track at a distance of 2.04 m, which is the length of each tram wheel circumference (Komorski et al., 2018). It means the one full wheel rotation period during the ride at a measuring distance was preserved, which was the most important measurement points selection criterion. Moreover, the minimum and maximum wheel diameter was about 600 and 654 mm, which is important in the case of wheel rotation frequency calculation. Furthermore, also photocells were used during the measurements for calculation of average tram speed.

### 3.3 Measurement devices and main recording parameters

The Brüel&Kjær equipment was used in the experimental research. The data acquisition module B&K type 3050-A-060 with 6 input was used. A tablet was used to control and monitor measurement process. All three B&K 4189-A-021 microphones are the first accuracy class microphones with a high measurement sensitivity equal to app. 50 mV/ms<sup>-2</sup>. Transducers were also calibrated before the acoustic measurement process.

The first main recording parameter was the measurement spectrum which was equal to 25.6 kHz. In the case of acoustic measurements this range should not be less than 20 kHz (Thompson, 2008); secondly, the high sampling frequency, which was about 65536 Hz. Therefore, the system provided high quality sound data where all signals were recorded synchronously. Duration of samples was dependent on the speed of the tram ride passing through the measurement cross section, and was about 5-7 s.

## 4 RESULTS AND ANALYSIS

The analyses began with the calculation of the frequency characteristic of the wheel surface damage discussed, based on the following formula:

$$f_{fp} = \frac{V}{c_w} [Hz] \tag{3}$$

where  $c_w$  [m] is the circumference of the wheel, and  $V$  [m/s] is the linear speed of the tram. Taking the circumference of the wheel into account requires the measurement of its actual diameter prior to analysing. To skip this, it was decided to simplify the method by introducing the rotational frequency search algorithm in the range of possible rotational frequencies ( $f_{wheel}$ ) for a particular speed. These ranges were determined from formula (3), taking into account possible travel speeds from 40 km/h to 20 km/h as well as extreme values of the wheel diameter. These values were measured during the research. The results are shown in Table 3.

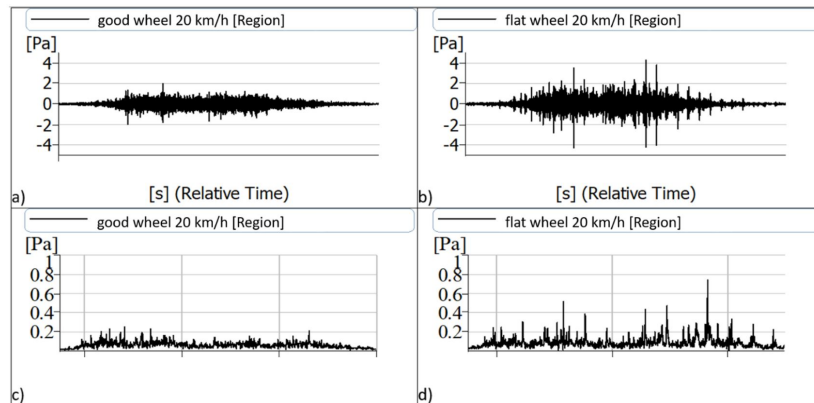
**Table 3** Ranges of possible rotational frequencies  $f_{wheel}$  for individual travel speeds and wheel diameters

Tram velocity \ Wheel diameter	max: 654 mm	min: 600 mm	$f_{wheel}$ [Hz]
40 km/h	5.41 Hz	5.89 Hz	<5.41; 5.89>
30 km/h	4.06 Hz	4.42 Hz	<4.06; 4.42>
20 km/h	2.71 Hz	2.95 Hz	<2.71; 2.95>

The algorithm works by finding a peak in a given frequency range  $f_{wheel}$ . Its location on the abscissa will testify to the diameter of the wheel. As presented in Table 3, due to travel speed, the rotational frequency for the first tested group

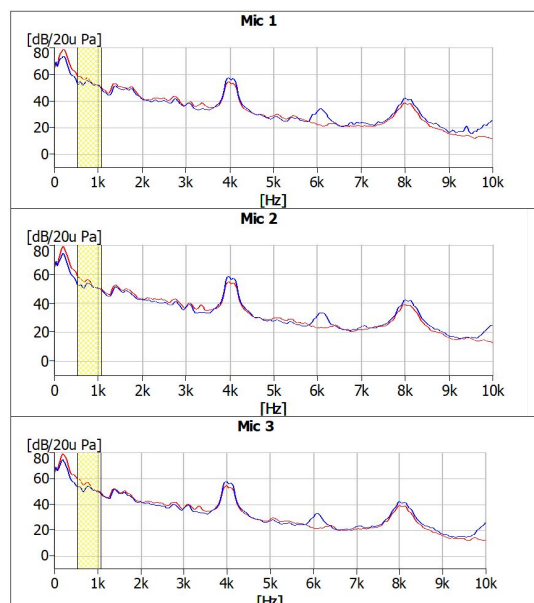
of vehicles will be in the range from 2.71 Hz to 2.95 Hz. However, for the second and third groups of objects studied, these frequencies will range from 4.06 to 4.42 Hz and 5.41 to 5.89 Hz, respectively.

Examples of the original sound samples are shown on the Figure 4 a-b (respectively; good and damage wheel). Moreover, there are also shown the envelopes (Figure 4 c-d) of the time history recordings. Based on the original signals' analyses, there were no opportunity to identify the frequencies mentioned in Table 3 because the full frequency range of the microphones is between 20-20 000 Hz. While the wheel flat damage generates cyclical impact noise at higher frequencies. Therefore, in case of seeking of the impact frequencies, authors carried out the envelope analysis using Hilbert transform. This process in details is described in the previous authors article (Nowakowski et al., 2019).



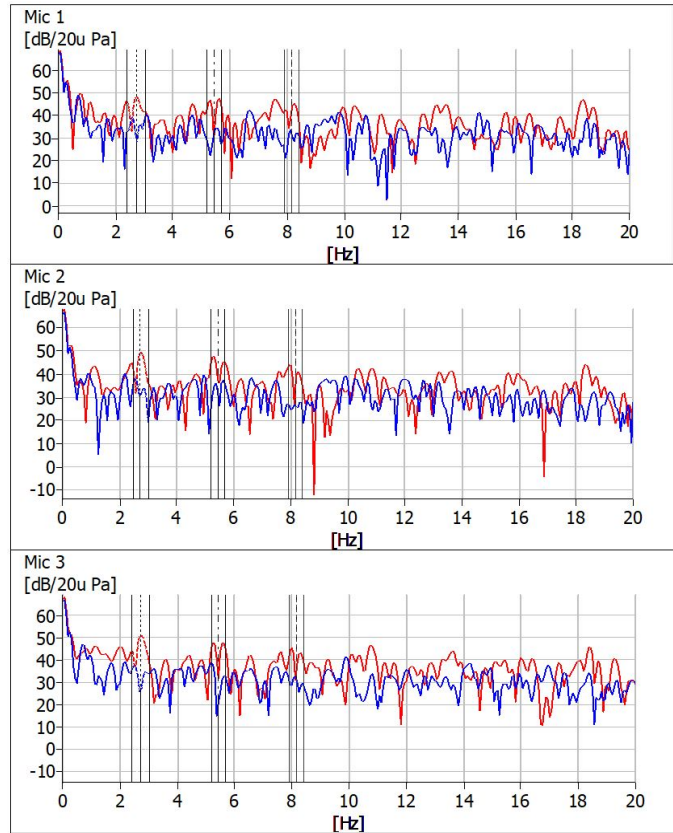
**Figure 4** Examples of original sound samples for 20 km/h speed (a – b) and their envelopes in time history (c – d)

Figure 5 shows the FFT spectra obtained from recorded sound pressure signals during the passage of sample trams without a flat wheel (blue) and with a flat wheel (red) at a speed of 20 km/h. Based in Figure 5 analysis, it was found that before performing envelope analysis, the signal should be filtered in the 800 Hz ± 500 Hz band. The indicated band is the result of analyses of changes in the dynamics of the observed measure. The analyses took into account relative differences between wheel states in the given 1 kHz bands and their differences after applying envelope analysis. The band with the highest dynamics in both presented aspects was selected. Analyses were performed in the range upwards from 400 Hz, ignoring the low-frequency components of rolling noise, up to 10 kHz taking into account the upper range of rolling noise (<5 kHz) and including accompanying tonal and impulse phenomena (Thompson, 2008). Observed higher sound levels at frequencies around 6 kHz could be generated by electrical equipment of tram running and motor system. Increased amplitudes could show abnormalities of their technical state, but in this case it requires further research area expanding.



**Figure 5** FFT sound pressure spectra (red – flat wheel; blue – good wheel) for 20 km/h speed from three microphones and two objects studied

Figure 6 shows the spectrum from acoustic signal envelopes (the instantaneous envelope is the amplitude of the complex Hilbert transform) with the first three harmonics rotational frequencies of the wheel (respectively marked;  $2.72 \text{ Hz} \pm 0.25 \text{ Hz}$ ,  $5.44 \text{ Hz} \pm 0.25 \text{ Hz}$ ,  $8.16 \pm 0.25 \text{ Hz}$ ), recorded with three microphones.



**Figure 6** Envelope spectra of sound pressure signals (red – flat wheel; blue – good wheel) with the first three rotational harmonic frequencies of the wheel (20 km/h)

Tables 4-6 present the results of calculating the RMS (Root Mean Square value) and maximum values in the spectrum from the acoustic signal envelopes in the  $2.72 \text{ Hz} \pm 0.25 \text{ Hz}$  (Table 4),  $5.44 \text{ Hz} \pm 0.25 \text{ Hz}$  (Table 5) and  $8.16 \text{ Hz} \pm 0.25 \text{ Hz}$  (Table 6) frequency bands.

**Table 4** Maximum values and RMS in the spectrum from the envelope in the  $2.72 \text{ Hz} \pm 0.25 \text{ Hz}$  for SPL measured at two different technical conditions of tram wheels

	Microphone 1		Microphone 2		Microphone 3	
	SPL <sub>RMS</sub> [dB]	SPL <sub>MAX</sub> [dB]	SPL <sub>RMS</sub> [dB]	SPL <sub>MAX</sub> [dB]	SPL <sub>RMS</sub> [dB]	SPL <sub>MAX</sub> [dB]
good wheel	43.8	39	42.1	38.4	41.8	37.5
flat wheel	52.7	48.2	53.2	49.4	55.2	51.1
difference	8.9	9.2	11.1	11	13.4	13.6

**Table 5** Maximum values and RMS in the envelope spectrum from the  $5.44 \text{ Hz} \pm 0.25 \text{ Hz}$  for SPL measured at two different technical conditions of the tram wheels

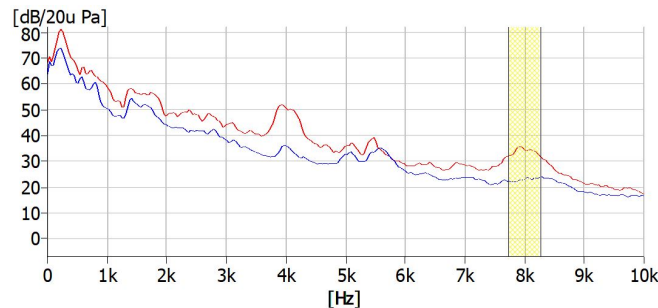
	Microphone 1		Microphone 2		Microphone 3	
	SPL <sub>RMS</sub> [dB]	SPL <sub>MAX</sub> [dB]	SPL <sub>RMS</sub> [dB]	SPL <sub>MAX</sub> [dB]	SPL <sub>RMS</sub> [dB]	SPL <sub>MAX</sub> [dB]
good wheel	39.4	36.4	42	37.4	39.5	37.9
flat wheel	52.6	47.6	52.5	47.7	53.3	47.7
difference	14.2	11.2	10.5	10.3	13.8	9.8

**Table 6** Maximum values and RMS in the spectrum from the envelope in the 8.16 Hz band ± 0.25 Hz for SPL measured at two different technical conditions of the tram wheels

	Microphone 1		Microphone 2		Microphone 3	
	SPL <sub>RMS</sub> [dB]	SPL <sub>MAX</sub> [dB]	SPL <sub>RMS</sub> [dB]	SPL <sub>MAX</sub> [dB]	SPL <sub>RMS</sub> [dB]	SPL <sub>MAX</sub> [dB]
good wheel	37.3	32.5	35.7	32.1	37.6	33.8
flat wheel	50.1	45.3	48.6	44.1	49.9	45.5
difference	12.8	12.8	12.9	12	12.3	11.7

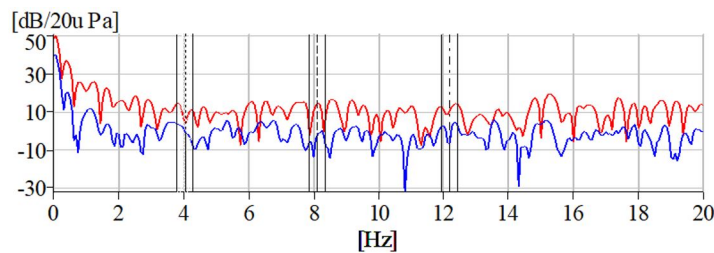
Based on the analysis of Figure 6 and Tables 4-6, it was found that for further research it is sufficient to use only one microphone, because the differences between the quantities describing the audio signal in the frequency domain did not exceed 3 dB. It was considered that both SPL<sub>RMS</sub> and SPL<sub>MAX</sub> calculated in bands related to the first three harmonics of the tram wheel rotational frequency can be used to detect wheel flats in urban rail vehicles. The sound pressure signal measured by microphone no. 1 was used for further analysis and processing.

Figure 7 shows the FFT spectra obtained from recorded sound pressure signals during passage of trams without a flat wheel (blue) and with a flat wheel (red) at a speed of 30 km/h.



**Figure 7** FFT sound pressure spectra (red – flat wheel; blue – good wheel) for the speed of 30 km/h

Based in Figure 7 analysis, it was found that before performing envelope analysis, the signal should be filtered in the 8 Hz ± 500 Hz band. The selection was made based on one of the visible resonance frequency ranges, while other bands were also checked (e.g. 800 Hz and 4 kHz), which also shows an increase in amplitude. Figure 8 shows the spectra of acoustic signal envelopes in the first three harmonics of the wheel rotational frequency 4.06 Hz ± 0.25 Hz, 8.13 Hz ± 0.25 Hz, 12.20 Hz ± 0.25 Hz marked, recorded at 30 km/h. Table 7 presents the results of calculations of RMS and maximum values in the spectrum from the acoustic signal envelope in the bands of the first three harmonic rotational frequencies of the wheel for measurements taken at a speed of 30 km/h.



**Figure 8** Acoustic signal envelope spectra (red – flat wheel; blue – good wheel) with the bands of first three rotational harmonic frequencies of the wheel marked (30 km/h)

**Table 7** Maximum values and RMS in the spectrum from the envelope in the bands of the first three rotational harmonic frequencies of the wheel for SPL measured at two different technical conditions of tram wheels

	1st harmonic		2nd harmonic		3rd harmonic	
	SPL <sub>RMS</sub> [dB]	SPL <sub>MAX</sub> [dB]	SPL <sub>RMS</sub> [dB]	SPL <sub>MAX</sub> [dB]	SPL <sub>RMS</sub> [dB]	SPL <sub>MAX</sub> [dB]
good wheel	9.6	4.2	4.3	0.2	9.5	4.6
flat wheel	19.4	14.7	19.5	14.8	20.2	14.6
difference	9.8	10.5	15.2	14.6	10.7	10

Figure 9 shows the FFT spectra obtained from recorded sound pressure signals during the passage of tram without a flat wheel (blue) and with a flat wheel (red) at a speed of 40 km/h.

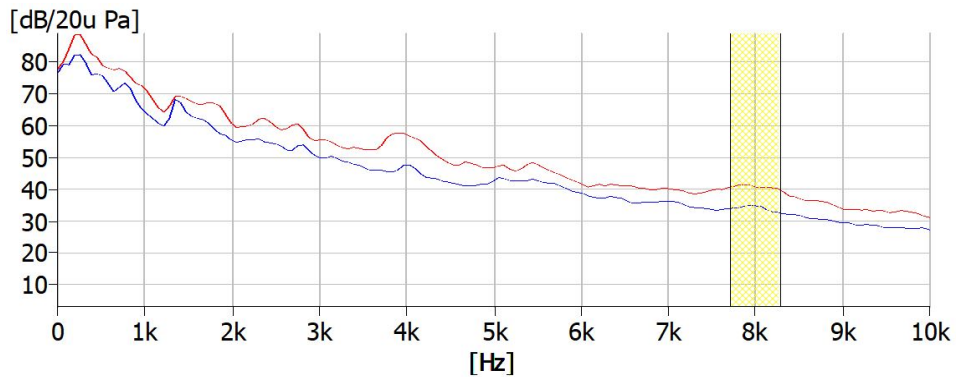


Figure 9 Spectrum of FFT sound pressure (red – flat wheel; blue – good wheel) for a speed of 40 km/h

Based in Figure 9 analysis, it was found that, as earlier, before performing envelope analysis, the signal should be filtered in the 8 Hz ± 500 Hz band. Figure 10 shows the spectra of acoustic signal envelopes with the band marked of the first three rotational harmonic frequencies of the wheel 5.44 Hz ± 0.25 Hz, 10.88 Hz ± 0.25 Hz, 16.32 Hz ± 0.25 Hz, recorded at a speed of 40 km/h.

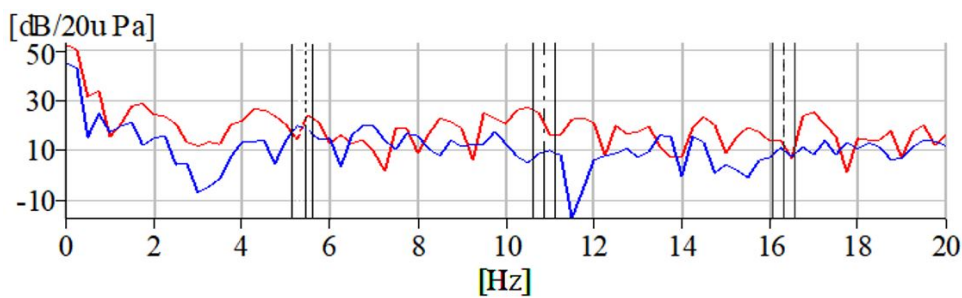


Figure 10 Spectrum of acoustic signal envelopes (red – flat wheel; blue – good wheel) with the marked band of the first three rotational harmonic frequencies of the wheel (40 km/h)

Table 8 presents the results of calculating the RMS and maximum values in the spectrum of the acoustic signal envelope in the bands of the first three harmonic rotational frequencies of the wheel for measurements taken at a travel speed of 40 km/h.

Table 8 Maximum values and RMS in the spectrum from the envelope in the bands of the first three rotational harmonic frequencies of the wheel for SPL measured at two different technical conditions of tram wheels

	1st harmonic		2nd harmonic		3rd harmonic	
	SPL <sub>RMS</sub> [dB]	SPL <sub>MAX</sub> [dB]	SPL <sub>RMS</sub> [dB]	SPL <sub>MAX</sub> [dB]	SPL <sub>RMS</sub> [dB]	SPL <sub>MAX</sub> [dB]
good wheel	21.7	20.1	12.5	10	15.3	14
flat wheel	25.7	24.3	28.1	27.4	26.7	25.4
difference	4	4.2	15.6	17.4	11.4	11.4

The data obtained in tests were analyzed in terms of the possibility of determining a point measure that meets the definition of the concept of diagnostic parameter. Sufficient width of the change field (sensitivity) was important in this respect. The average difference  $\bar{x}_a$  between the values characterizing a good wheel and a flat wheel within the analyzed speeds was calculated for all other measures. The second value was the coefficient of variation of  $CV_{\bar{x}_a}$  of this difference. The choice of measure determined the criterion of the maximum average difference with the minimum coefficient of its variability characterized by the maximum quotient of these values. The results are summarized in Table 9.

**Table 9** Values  $\bar{x}_a$   $CV_{\bar{x}_a}$  and their quotient for cases analyzed

	$\bar{x}_a$ [dB]	$CV_{\bar{x}_a}$ [%]	$\bar{x}_a / CV_{\bar{x}_a}$
SPL <sub>RMS</sub> , 1st harmonic	7.4	41.0	0.2
SPL <sub>RMS</sub> , 2nd harmonic	14.7	8.8	1.7
SPL <sub>RMS</sub> , 3d harmonic	11.6	9.2	1.3
SPL <sub>MAX</sub> , 1st harmonic	8.0	41.8	0.2
SPL <sub>MAX</sub> , 2nd harmonic	14.4	21.6	0.7
SPL <sub>MAX</sub> , 3rd harmonic	11.4	1.4	8.1

In accordance with the data presented, the best diagnostic parameter seems to be SPL<sub>MAX</sub> calculated for the third harmonic rotational speed of the wheel. Detailed results for this measure are shown in Figure 11.

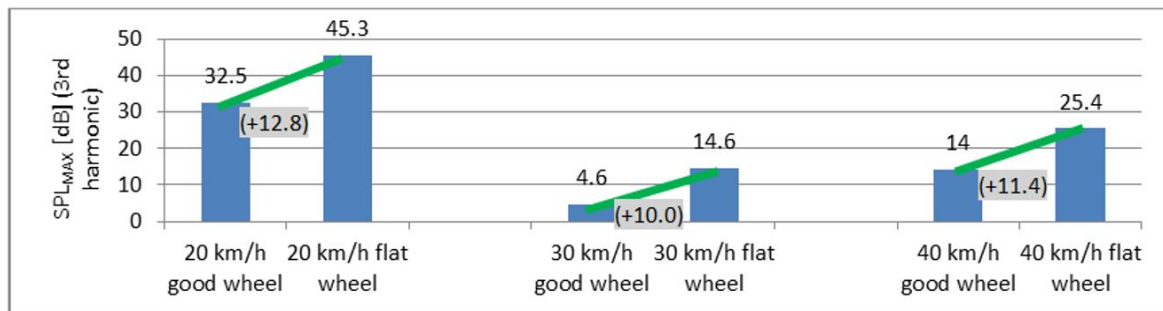


**Figure 11** SPL<sub>MAX</sub> calculated from the third wheel harmonic rotational speed for the passes analyzed

The indicated SPL<sub>MAX</sub> measure was higher in the case of a wheel flat at 13 dB for the speed of 20 km/h, and over 15 dB for other speeds. Limit values should be determined individually by a given rolling stock operator, taking into account the correlation between limit values and wheel speed. In vibroacoustic diagnostics it is assumed that a change in the technical condition of the machine is indicated by a 6-decibel increase or by a decrease in the diagnostic parameter (Cempel, 1993; Niziński and Michalski, 2002). Based on the analysis of Tables 7-9 and Figure 11, it was found that both SPL<sub>RMS</sub> and SPL<sub>MAX</sub> calculated in the bands associated with the first three harmonic rotational frequencies of the tram wheel can be used to detect flat spots on the wheels of urban rail vehicles moving at a speed of 20 km/h and 30 km/h. In the case of testing trams travelling at a speed of 40 km/h, it can be used to detect a flat wheel on the SPL<sub>RMS</sub> and SPL<sub>MAX</sub> wheels for the second and third harmonic rotational frequencies of the tram wheels.

### 5 DISCUSSION

Nowadays the acoustic signal processing in railway field, especially in case of wayside wheel-flat detection system, is not a popular solution. In comparison to other railway scientific articles, more often authors use the vibration signal measured on the axle box or bogie frames to elaborate the vehicle (or rail) monitoring damage system, as in (García-Macías and Martínez-Castro, 2020; Kim et al., 2020). They have shown important estimation of dynamic response in time and frequency range during vehicle passage through the rail infrastructure. The Hilbert and Fourier transforms (and also other processing methods) in these two articles are used with significant efficiency in overall result. Furthermore, in other scientific fields the acoustic impact (or impulse) processing is also very popular way to achieve the irregularity detection system goal. In (Batrakov et al., 2010; Fan and Zuo, 2006; Raja et al., 2013; Sun et al., 2014) authors have shown that Hilbert transform is a proper calculation method to extract the important information from sound signals in different scientific fields. Therefore, signal modulation or decomposition process in most research cases was performed using different methodology fitted to the each case study. The main article novelty in contrast to other scientific positions is estimation of the diagnostic parameters (SPL<sub>RMS</sub> and SPL<sub>MAX</sub>) for the second and third rotational harmonic frequencies of the wheel (using acoustic signals processing, not vibration). These two point measures were selected based on proposed calculation method. What is more important, there are significant differences in dynamics of selected parameters (between good and damage cases) thankful to signal demodulation process. Therefore, extraction of the diagnostic information by proposed analysis steps was accomplished.

## 6 CONCLUSIONS

The article presents the possibility of using acoustic signals to diagnose rail vehicle wheels in the context of detecting defects in rolling surfaces such as wheel-flats. The procedure described uses a method based on Hilbert transform and spectrum analysis of acoustic signal envelopes.

Based on the tests carried out, it was found that the acoustic signal recorded in close proximity to a passing rail vehicle is a very good carrier of diagnostic information regarding the detection of flat wheels. The determined point measures in the form of sound pressure levels MAX and RMS meet the requirements of diagnostic parameters taking into account their dependence on travel speed. The highest sensitivity at the level of 13-15 dB was obtained by analyzing the parameters for the second and third basic rotational harmonic frequencies of the wheel. The tests were carried out in the 20-40 km/h speed range, which is in line with the actual speed range of trams in tram depots. In addition, it seems that a better solution is to implement the diagnostic process for lower speeds due to Heisenberg uncertainty principle. Limit values of diagnostic parameters indicated should be determined individually by a given rolling stock operator depending on tram speeds. It is necessary to correlate these values to global costs of removing damage detected in the estimation of external transport costs.

In addition, research shows that it is possible to reduce the measurement points to one, which may contribute to reducing the total costs of building a diagnostic system. The method proposed can be complementary to existing trackside diagnostic systems installed in rail vehicle depots. The microphone can be one of measuring elements, also used to determine technical conditions of other components, e.g. running gear noise or detection of undesirable rattle noise of elements that have worked loose. In this aspect, it is the direction of further research for the authors of this paper.

## Acknowledgements

All presented work is partly funded by Statutory Activities fund of the Institute of Transport, PUT (PL) 0416/SBAD/0295 and 0416/SBAD/0001. Thanks to the Municipal Communication Company in Poznan for the possibility of carrying out measurements at the Franowo depot.

**Author's Contributions:** Conceptualization, P Komorski, GM Szymanski, T Nowakowski; Formal Analysis, GM Szymanski, T Nowakowski; Methodology, P Komorski, GM Szymanski, T Nowakowski; Investigation, P Komorski, T Nowakowski; Writing - original draft, P Komorski, T Nowakowski; Writing - review & editing, P Komorski, GM Szymanski, T Nowakowski; Funding acquisition, M Orczyk; Resources, M Orczyk; Supervision, P Komorski.

**Editor:** Jan Awrejcewicz.

## References

- Alemi, A., Corman, F. and Lodewijks, G. (2016). Review on condition monitoring approaches for the detection of railway wheel defects. *Proceedings of the Institution of Mechanical Engineers, Part F: Journal of Rail and Rapid Transit*, 0(0), 1–21. <https://doi.org/10.1177/0954409716656218>
- Alexandrou, G., Kouroussis, G. and Verlinden, O. (2016). A comprehensive prediction model for vehicle/track/soil dynamic response due to wheel flats. *Proceedings of the Institution of Mechanical Engineers, Proc. IMechE Part F: Journal of Rail and Rapid Transit*, 230(4), 1088–1104. <https://doi.org/10.1177/0954409715576015>
- Batrkov, D. O., Golovin, D. V., Simachev, A. A. and Batrkova, A. G. (2010). Hilbert transform application to the impulse signal processing. *2010 5th International Conference on Ultrawideband and Ultrashort Impulse Signals, UWBUSIS'2010*, 113–115. <https://doi.org/10.1109/UWBUSIS.2010.5609110>
- Behr, W. (2013). *Definition of wheel maintenance measures for reducing ground vibration. RIVAS project D2.7.*
- Belotti, V., Crenna, F., Michelini, R. C. and Rossi, G. B. (2006). Wheel-flat diagnostic tool via wavelet transform. *Mechanical Systems and Signal Processing*, 20(8), 1953–1966. <https://doi.org/10.1016/j.ymssp.2005.12.012>
- Bracciali, A., Lionetti, G. and Pieralli, M. (1997). Effective wheel flats detection through a simple device. *World Congress on Railway Research WCRR, 97*, 513–521.

- Brizuela, J., Fritsch, C. and Ibáñez, A. (2011). Railway wheel-flat detection and measurement by ultrasound. *Transportation Research Part C: Emerging Technologies*, 19(6), 975–984. <https://doi.org/10.1016/j.trc.2011.04.004>
- Brizuela, Jose, Ibañez, A., Nevado, P. and Fritsch, C. (2010). Railway wheels flat detector using doppler effect. *Physics Procedia*, 3(1), 811–817. <https://doi.org/10.1016/j.phpro.2010.01.104>
- Cempel, C. (1993). *Vibroacoustic condition monitoring (Ellis Horwood Series in Mechanical Engineering)*. (S. D. Haddad, Ed.). Warsaw: Ellis Horwood.
- Fan, X. and Zuo, M. J. (2006). Gearbox fault detection using Hilbert and wavelet packet transform. *Mechanical Systems and Signal Processing*, 20(4), 966–982. <https://doi.org/10.1016/j.ymsp.2005.08.032>
- Feldman, M. (2011). Hilbert transform in vibration analysis. *Mechanical Systems and Signal Processing*, 25(3), 735–802. <https://doi.org/10.1016/j.ymsp.2010.07.018>
- García-Macías, E. and Martínez-Castro, A. E. (2020). Hilbert transform-based semi-analytic meta-model for maximum response envelopes in dynamics of railway bridges. *Journal of Sound and Vibration*, 487, 115618. <https://doi.org/10.1016/j.jsv.2020.115618>
- Jia, S. and Dhanasekar, M. (2007). Detection of Rail Wheel Flats using Wavelet Approaches. *Structural Health Monitoring: An International Journal*. <https://doi.org/10.1177/1475921706072066>
- Jing, L. (2018). Wheel-Rail Impact by a Wheel Flat. In A. Hessami (Ed.), *Modern Railway Engineering*. <https://doi.org/10.5772/68005>
- Kim, E., Jayaprakasam, N., Cui, Y. and Martin, U. (2020). Defect Prediction of Railway Wheel Flats based on Hilbert Transform and Wavelet Packet Decomposition. *Electrical Engineering and Systems Science*, 1–24.
- Komorski, P., Nowakowski, T., Szymanski, G. M. and Tomaszewski, F. (2018). Application of Time-Frequency Analysis of Acoustic Signal to Detecting Flat Places on the Rolling Surface of a Tram Wheel. In *Springer Proceedings in Mathematics and Statistics* (Vol. 249). [https://doi.org/10.1007/978-3-319-96601-4\\_19](https://doi.org/10.1007/978-3-319-96601-4_19)
- Komorski, P., Szymanski, G. M., Nowakowski, T. and Orczyk, M. (2019). Application of the wheel-flat detection algorithm using advanced acoustic signal analysis. In J. Awrejcewicz, M. Kaźmierczak, & J. Mrozowski (Eds.), *Theoretical Approaches in Non-Linear Dynamical Systems DSTA 2019* (pp. 269–278). Łódź (Poland): Wydawnictwo Politechniki Łódzkiej.
- Kouroussis, G., Alexandrou, G., Connolly, D., Vogiatzis, K. and Verlinden, O. (2015). Railway-induced ground vibrations in the presence of local track irregularities and wheel flats. In *5th International Conference on Computational Methods in Structural Dynamics and Earthquake Engineering Methods in Structural Dynamics and Earthquake Engineering* (pp. 26–37). Crete, Greece.
- Krummenacher, G., Ong, C. S., Koller, S., Kobayashi, S., Buhmann, J. M. and Member, S. (2017). Wheel Defect Detection With Machine Learning, 1–12.
- Li, Y., Zuo, M. J., Lin, J. and Liu, J. (2017). Fault detection method for railway wheel flat using an adaptive multiscale morphological filter. *Mechanical Systems and Signal Processing*, 84, 642–658. <https://doi.org/10.1016/j.ymsp.2016.07.009>
- Liang, B., Iwnicki, S., Feng, G., Ball, A., Tran, V. T. and Cattley, R. (2013). Railway wheel flat and rail surface defect detection by time-frequency analysis. *Chemical Engineering Transactions*, 33, 745–750. <https://doi.org/10.3303/CET1333125>
- Luo, H., Fang, X. and Ertas, B. (2009). Hilbert Transform and Its Engineering Applications. *AIAA Journal*, 47(4), 923–932. <https://doi.org/10.2514/1.37649>
- Madejski, J. (2006). Automatic detection of flats on the rolling stock wheels. *Journal of Achievements in Materials and ...*, 16(1), 160–163. Retrieved from [http://www.w.journalamme.org/papers\\_cams05/1204.pdf](http://www.w.journalamme.org/papers_cams05/1204.pdf)
- Meixedo, A., Gonçalves, A., Calçada, R., Gabriel, J., Fonseca, H. and Martins, R. (2015). Weighing in motion and wheel defect detection of rolling stock. In *2015 3rd Experiment International Conference (exp.at'15)*. Ponta Delgada (Portugal): IEEE. <https://doi.org/10.1109/EXPAT.2015.7463220>
- Niziński, S. and Michalski, R. (2002). *Diagnostyka obiektów technicznych (ang. Diagnostics of technical objects)*. Radom (Polska): Instytut Technologii Eksploatacji.
- Nowakowski, T., Komorski, P., Szymański, G. M. and Tomaszewski, F. (2019). Wheel-flat detection on trams using envelope analysis with Hilbert transform. *Latin American Journal of Solids and Structures*, 16(1). <https://doi.org/10.1590/1679-78255010>

- Polish National Railways Directorate. Mw-2 Instruction: The technical maintenance principles of standard gauge freight wagons. Permissible wear of parts and sets of freight wagons. (2000).
- Raja, J. E., Kiong, L. C. and Soong, L. W. (2013). Hilbert-Huang Transform-Based Emitted Sound Signal Analysis for Tool Flank Wear Monitoring. *Arabian Journal for Science and Engineering*, 38(8), 2219–2226. <https://doi.org/10.1007/s13369-013-0580-7>
- Roveri, N., Carcaterra, A. and Sestieri, A. (2015). Real-time monitoring of railway infrastructures using fibre Bragg grating sensors. *Mechanical Systems and Signal Processing*, 60, 14–28. <https://doi.org/10.1016/j.ymssp.2015.01.003>
- Skudrzyk, E. (1971). *The Foundations of Acoustics*. Vienna: Springer Vienna. <https://doi.org/10.1007/978-3-7091-8255-0>
- Standard. EN 15313:2016. Railway applications. In-service wheelset operation requirements. In-service and off-vehicle wheelset maintenance (2016).
- Standard. EN 14811:2019. Railway applications - Track - Special rails - Grooved rails and related structural profiles (2019).
- Stypuła, K. (2001). *Drgania mechaniczne wywołane eksploatacją metra płytkiego i ich wpływ na budynki (ang. Mechanical vibrations caused by underground operation and their impact on buildings)*. Cracow: Publishing house of the Cracow University of Technology.
- Sun, S., Jiang, Z., Wang, H. and Fang, Y. (2014). Automatic moment segmentation and peak detection analysis of heart sound pattern via short-time modified Hilbert transform. *Computer Methods and Programs in Biomedicine*, 114(3), 219–230. <https://doi.org/10.1016/j.cmpb.2014.02.004>
- Thompson, D. J. (1996). On the relationship between wheel and rail surface roughness and rolling noise. *Journal of Sound and Vibration*, 193(1), 149–160. <https://doi.org/10.1006/jsvi.1996.0254>
- Thompson, D. J. (2008). *Railway Noise And Vibration: Mechanisms, Modelling and Means of Control* (1st ed.). Southampton: Elsevier.
- Tomlinson, G. R. (1987). Developments in the use of the Hilbert transform for detecting and quantifying non-linearity associated with frequency response functions. *Mechanical Systems and Signal Processing*, 1(2), 151–171. [https://doi.org/10.1016/0888-3270\(87\)90068-9](https://doi.org/10.1016/0888-3270(87)90068-9)
- Wu, T. X. and Thompson, D. J. (2003). On the impact noise generation due to a wheel passing over rail joints. *Journal of Sound and Vibration*, 267(3), 485–496. [https://doi.org/10.1016/S0022-460X\(03\)00709-0](https://doi.org/10.1016/S0022-460X(03)00709-0)
- Zhang, D., Entezami, M., Stewart, E., Roberts, C. and Yu, D. (2018). Adaptive fault feature extraction from wayside acoustic signals from train bearings. *Journal of Sound and Vibration*, 425, 221–238. <https://doi.org/10.1016/j.jsv.2018.04.004>